Electronic Supplementary Material (ESI) for Biomaterials Science.

Supporting Information

Hollow Ferric-Tannic Acid Nanocapsules with Sustained O_2 and ROS Induction for Synergistic Tumor Therapy

[a] *State Key Laboratory of Silicon Materials, School of Materials Science and Engineering, Zhejiang University, Hangzhou 310027, P.R. China*

[b] *Department of Surgery, Second Affiliated Hospital, Zhejiang University School of Medicine, Zhejiang University, Hangzhou, 310000, P. R. China*

† Authors with equal contribution

*Corresponding authors: xiang.li@zju.edu.cn (XL)

Huimin Zhu, [†a] Guodong Cao, [†b] Chu Qiang, [a] YiKe Fu, [a] Yulian Wu, [b] Xiang Li *[a] and Gaorong Han [a]

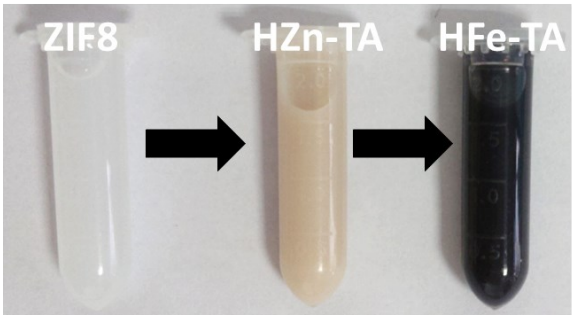

Figure S1. The color of ZIF8, HZn-TA and HFe-TA solutions during synthetic process.

Table S1. The surface area, pore volume and pore size of HFe-TA nanoparticles.

Surface area $[m^2g^{-1}]$	Pore volume $[cm^3g^{-1}]$	Pore size [nm]
~45.1	~0.2	~19.2

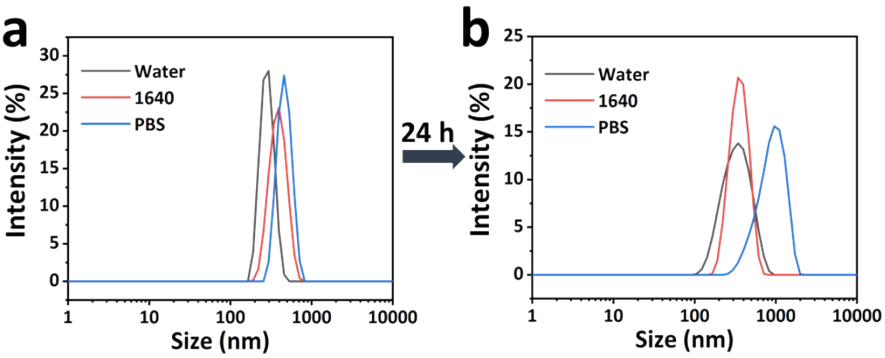

Figure S2. Size distribution of HFe-TA nanocapsules in water, 1640 (containing 10% fetal bovine serum), and PBS for (a) 0 h and (b) 24 h.

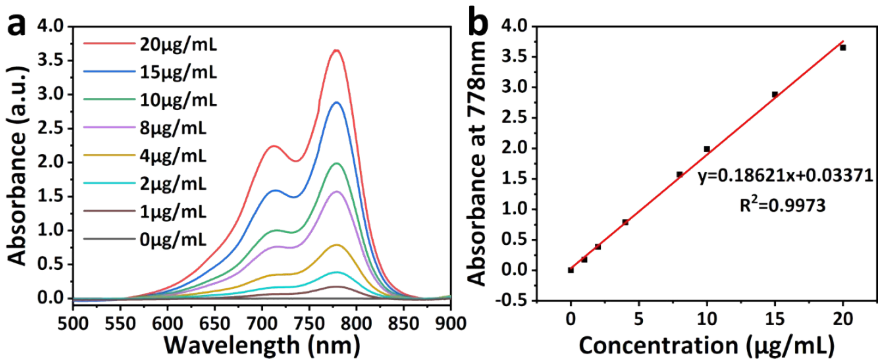

Figure S3. (a) UV–vis absorbance spectra of ICG in water with different concentrations, and (b) the ICG standard curve of absorbance at 778 nm.

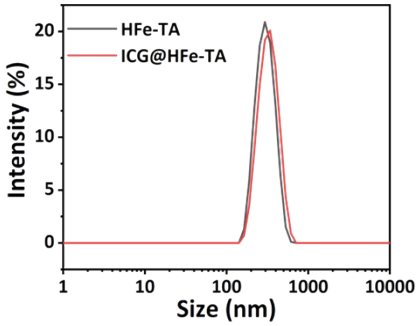

Figure S4. (a) Size distribution of HFe-TA and ICG@HFe-TA.

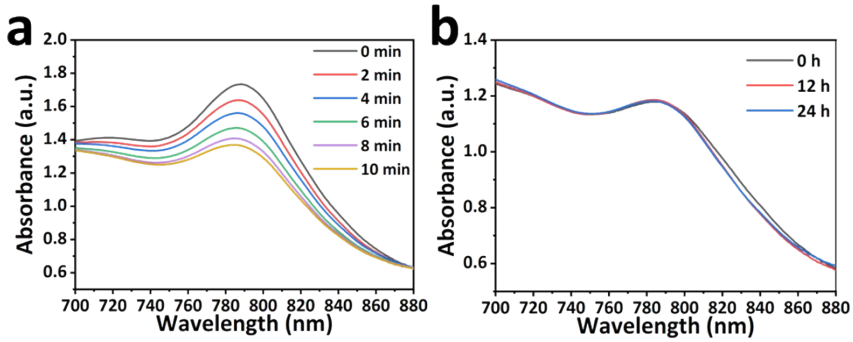

Figure S5. Absorbance of ICG (a) with different irradiation time and (b) without irradiation for ICG@HFe-TA.

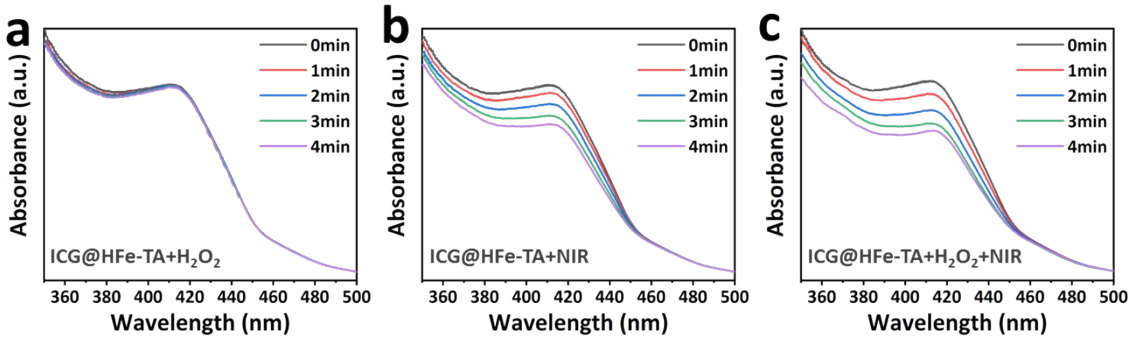

Figure S6. Time-dependent depletion of DPBF due to $^1O_2$ generation: (a) 200 μg mL^{-1} of ICG@HFe-TA with 250μM H_2O_2, (B) 200 μg mL^{-1} of ICG@HFe-TA with 808 nm laser (1.5 W cm^{-2}). (c) 200 μg mL^{-1} of ICG@HFe-TA with 250μM H_2O_2 and 808 nm laser (1.5 W cm^{-2}).

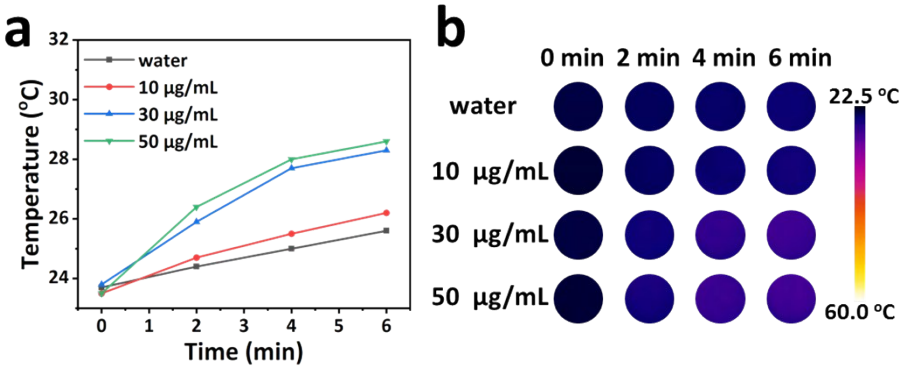

Figure S7. (a) Curves and (b) photographs of temperature variation of ICG@HFe-TA solutions with different concentrations under 808nm-NIR irradiation for varied period.

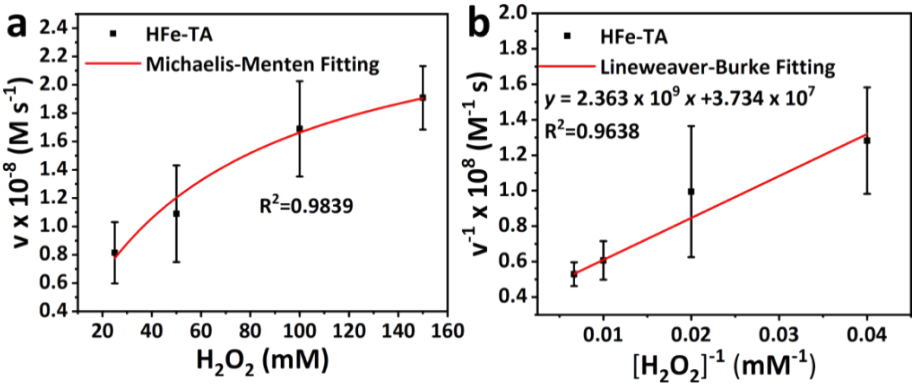

Figure S8. (a)The Michaelis-Menten fitting curves of initial hydroxyl radical generation velocities versus H_2O_2 concentration. (b) The Lineweaver-Burke fitting (double reciprocal) of Michaelis-Menten fitting curve. (Mean values and error bars are defined as mean and s.d. , respectively.)

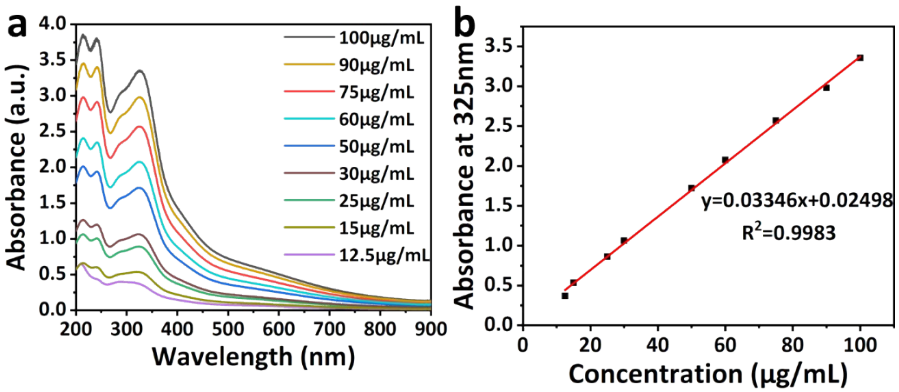

Figure S9. (a) UV–vis absorbance spectra of HFe-TA in water with different concentrations, and (b) the HFe-TA standard curve of absorbance at 325 nm.

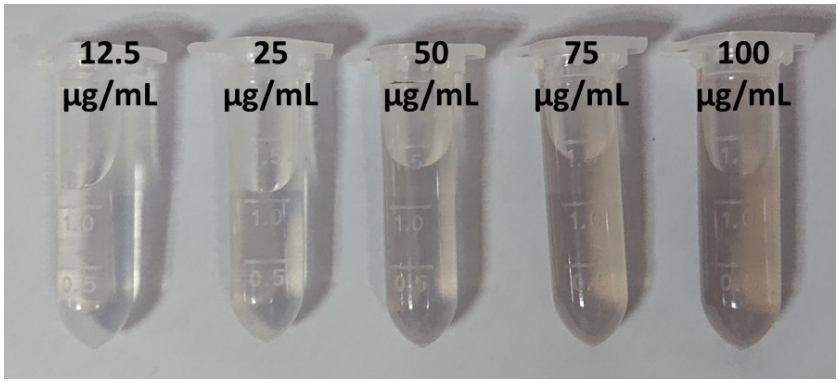

Figure S10. Digital photographs of different concentrations of HFe-TA solutions.

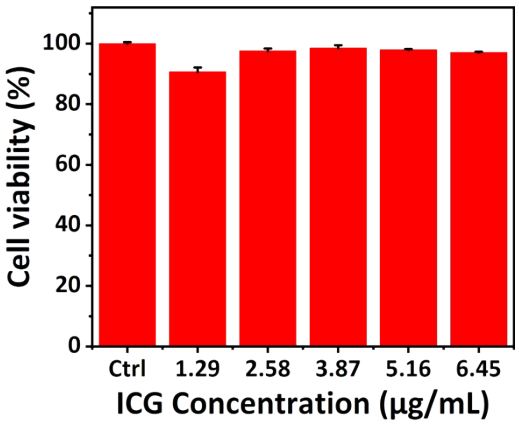

Figure S11. 4T1 cells viability incubated with different concentrations of ICG.

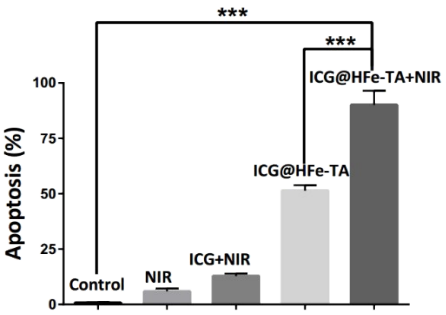

Figure S12. The bar graph presents the percentage of apoptotic cells. The experiments were performed in triplicate; the data are expressed as the mean ± standard deviation. *** P<0.001

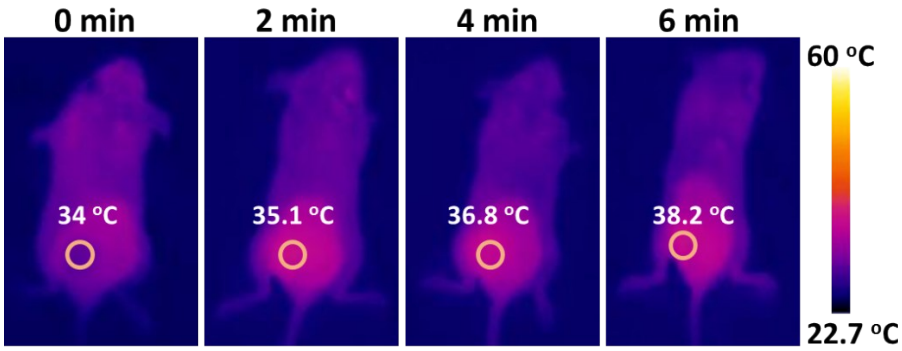

Figure S13. Infrared thermographic images of mice bearing tumor treated with ICG@HFe-TA after 4h intratumoral injection under 808nm-NIR irradiation.

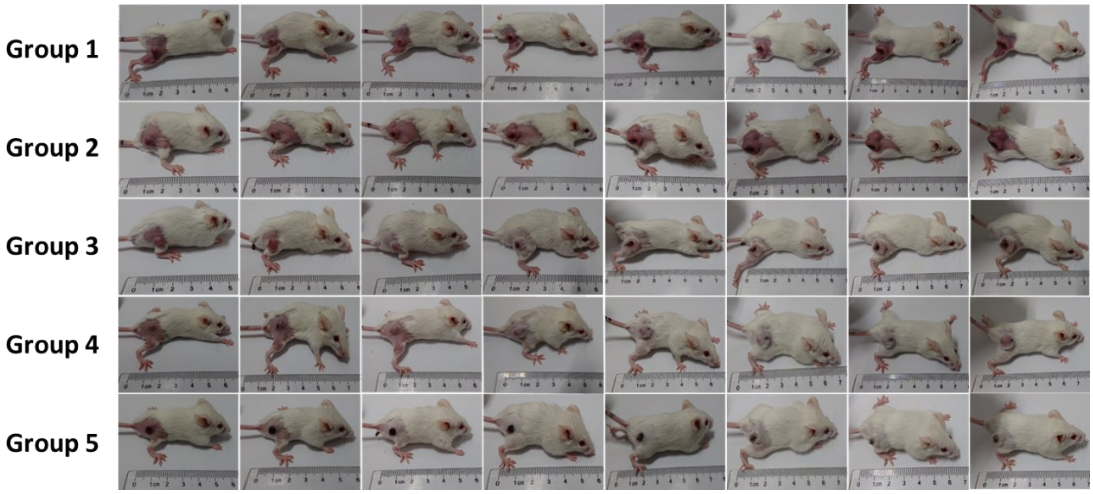

Figure S14. Images of 4T1 tumor-bearing Balb/c mice of each group on every 2-day in 14 days receiving various treatments.

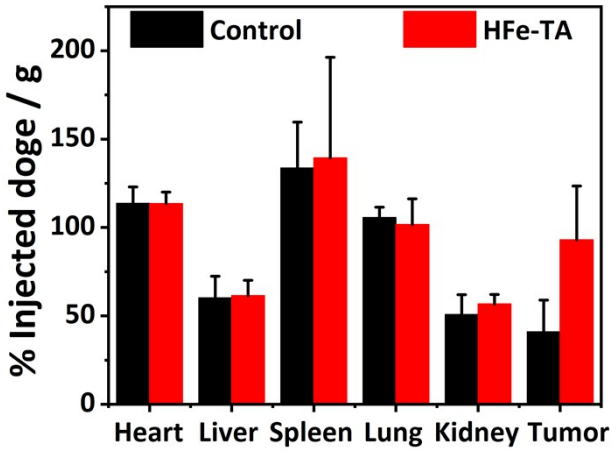

Figure S15. The biodistribution of Fe (% injected dose of Fe per gram of tissues) in main organs and tumor after injection for 24 h.